

# The Crystal Structure and Electronic Properties of the Complexes Acetatobis(1,10-phenanthroline)copper(II) Perchlorate Dihydrate, Acetatobis(1,10-phenanthroline)copper(II) Nitrate Dihydrate, and Acetatobis(1,10-phenanthroline)zinc(II) Tetrafluoroborate Dihydrate †

William Fitzgerald and Brian Hathaway\*

The Chemistry Department, University College Cork, Ireland

Charles J. Simmons

The Chemistry Department, University of Puerto Rico, Rio Piedras Campus, Puerto Rico 00931

The crystal structure of  $[\text{Cu}(\text{phen})_2(\text{O}_2\text{CMe})][\text{ClO}_4]\cdot 2\text{H}_2\text{O}$  (1),  $[\text{Cu}(\text{phen})_2(\text{O}_2\text{CMe})][\text{NO}_3]\cdot 2\text{H}_2\text{O}$  (2), and  $[\text{Zn}(\text{phen})_2(\text{O}_2\text{CMe})][\text{BF}_4]\cdot 2\text{H}_2\text{O}$  (3) have been determined by X-ray analysis. Complex (1) crystallises in the monoclinic space group  $P2_1/c$  with  $a = 9.671(3)$ ,  $b = 8.282(3)$ ,  $c = 17.595(4)$  Å,  $\beta = 109.63(2)^\circ$ , and  $Z = 2$ ; (2) crystallises in the triclinic space group  $P\bar{1}$  with  $a = 14.728(2)$ ,  $b = 10.499(2)$ ,  $c = 8.603(2)$  Å,  $\alpha = 104.19(5)$ ,  $\beta = 83.97(5)$ ,  $\gamma = 96.81(5)^\circ$ , and  $Z = 2$ ; (3) crystallises in the monoclinic space group  $P2_1/c$  with  $a = 9.659(2)$ ,  $b = 8.262(2)$ ,  $c = 17.651(2)$  Å,  $\beta = 109.06(5)^\circ$ , and  $Z = 2$ . The  $\text{MN}_4\text{O}_2$  chromophore in all three complexes has a *cis*-octahedral stereochemistry. In (1) and (3) the metal atoms have  $C_2$  symmetry and in (1) there is a marked *cis* distortion of the Cu–O distances. In (2) a distortion of the  $\text{CuN}_4\text{O}_2$  chromophore towards a square pyramidal ( $4 + 1 + 1^*$ ) stereochemistry is present. The polycrystalline e.s.r. spectra of (1) and (2) and of 10% copper(II)-doped (3) are temperature variable, consistent with a fluxional  $\text{CuN}_4\text{O}_2$  chromophore stereochemistry. The temperature variability of the single-crystal e.s.r. spectra of (1), (2), and copper(II)-doped (3) is restricted to the  $\text{CuN}_2\text{O}_2$  plane, consistent with two-dimensional fluxional behaviour. The electronic reflectance spectra of (1) and (2) involve two peaks at *ca.* 10 000 and *ca.* 14 000  $\text{cm}^{-1}$  and relate to the underlying static  $\text{CuN}_4\text{O}_2$  ( $4 + 1 + 1^*$ ) chromophore stereochemistry.

The recent determination,<sup>1,2</sup> of the low-temperature crystal structures of  $[\text{Cu}(\text{bipy})_2(\text{ONO})][\text{NO}_3]$  (4) (bipy = 2,2'-bipyridyl) at 298, 165, 100, and 20 K have established the fluxional behaviour<sup>3</sup> of the  $\text{CuN}_4\text{O}_2$  chromophore as predicted earlier<sup>4</sup> from the limited temperature-variable e.s.r. spectra of (4), and particularly the copper(II)-doped  $[\text{Zn}(\text{bipy})_2(\text{ONO})][\text{NO}_3]$  system. As the e.s.r. spectra,<sup>5</sup> of a series of four cation distortion isomers  $[\text{Cu}(\text{phen})_2(\text{O}_2\text{CMe})\text{Y}]$  ( $\text{Y} = \text{BF}_4^-\cdot 2\text{H}_2\text{O}$ ,  $\text{ClO}_4^-\cdot 2\text{H}_2\text{O}$ ,  $\text{BF}_4^-$ , or  $\text{ClO}_4^-$ ) have been reported to be temperature variable, the  $\text{CuN}_4\text{O}_2$  chromophores of these isomers were predicted to be fluxional. This has been confirmed,<sup>6</sup> by the recent low-temperature (173 K) crystal structure of  $[\text{Cu}(\text{phen})_2(\text{O}_2\text{CMe})][\text{ClO}_4]$  (phen = 1,10-phenanthroline). The present paper reports the crystal structures of the complexes  $[\text{Cu}(\text{phen})_2(\text{O}_2\text{CMe})][\text{ClO}_4]\cdot 2\text{H}_2\text{O}$  (1),  $[\text{Cu}(\text{phen})_2(\text{O}_2\text{CMe})][\text{NO}_3]\cdot 2\text{H}_2\text{O}$  (2), and  $[\text{Zn}(\text{phen})_2(\text{O}_2\text{CMe})][\text{BF}_4]\cdot 2\text{H}_2\text{O}$  (3), the e.s.r. spectra of (1), (2), and of copper(II)-doped (3).

## Experimental

**Preparations.**—Complex (1) was prepared,<sup>5</sup> by adding 1,10-phenanthroline monohydrate (0.5 g, 2.52 mmol) in water–acetone (1:1, 20  $\text{cm}^3$ ) to  $[\text{Cu}(\text{OH}_2)_6][\text{ClO}_4]_2$  (0.47 g, 1.26 mmol) in water–acetone (1:1, 20  $\text{cm}^3$ ). The solution was then boiled and  $\text{Na}(\text{O}_2\text{CMe})\cdot 3\text{H}_2\text{O}$  (0.686 g, 5.02 mmol) in water (10  $\text{cm}^3$ ) was added. The light blue solution was diluted to 500  $\text{cm}^3$  with water, boiled, filtered, and allowed to stand at room temperature; light blue crystals of (1) were deposited after several weeks (Found: C, 51.15; H, 3.45; Cl, 6.10; Cu,

10.75; N, 9.20.  $\text{C}_{26}\text{H}_{23}\text{ClCuN}_4\text{O}_8$  requires C, 50.5; H, 3.70; Cl, 5.75; Cu, 10.3; N, 9.05%). Complex (2) was prepared by a similar method using  $[\text{Cu}(\text{OH}_2)_6(\text{NO}_3)_2]$  (Found: C, 53.5; H, 4.00; Cu, 11.1; N, 12.05.  $\text{C}_{26}\text{H}_{23}\text{CuN}_5\text{O}_7$  requires C, 53.75; H, 4.00; Cu, 10.95; N, 12.05%). Complex (3) was prepared by a similar method using  $[\text{Zn}(\text{OH}_2)_6][\text{BF}_4]_2$  (Found: C, 51.5; H, 3.35; N, 9.20.  $\text{C}_{26}\text{H}_{23}\text{BF}_4\text{N}_4\text{O}_4\text{Zn}$  requires C, 51.4; H, 3.80; N, 9.20%).

**Crystallography.**—The crystallographic data for (1), (2), and (3) are summarised in Table 1. For all three complexes, the preliminary unit-cell data and space groups were determined from precession photographs and refined on a Philips PW1100 four-circle diffractometer. The intensities were collected on the diffractometer with graphite-monochromatised Mo- $K_\alpha$  radiation; an  $\theta$ - $2\theta$  scan mode was used and reflections with  $3 < \theta < 25$ , 30, and  $32^\circ$ , for (1), (2), and (3), respectively in one quadrant were examined. A constant scan speed of  $0.05^\circ \text{ s}^{-1}$  was used with a variable scan width of  $(0.7 + 0.1 \tan \theta)^\circ$ ; the acceptance criterion  $I > 2.5\sigma(I)$  was used. Lorentz and polarisation corrections were applied, but no correction was made for absorption or extinction.

The structures were solved by Patterson and Fourier techniques and refined by full-matrix least-squares analysis, with anisotropic thermal parameters for all the non-hydrogen atoms. The positions of the hydrogen atoms were calculated geometrically with C–H 1.08 Å and a fixed thermal parameter of  $0.07 \text{ \AA}^2$  and floated on the associated C atom. A refined weighting scheme was used with  $w = k/[\sigma^2(F_o) + g(F_o)^2]$  (see Table 1 for the final values of  $k$  and  $g$ ) and the refinements converged when the final shift to error ratio was  $< 0.005$  in all three complexes, see Table 1. Complex neutral scattering factors<sup>7</sup> were used for the non-hydrogen atoms and those for the heavy atoms were corrected for anomalous dispersion. In both (1) and (3) the  $\text{ClO}_4^-$  and  $\text{BF}_4^-$  anions occupied special positions of two-fold symmetry; attempts to refine these

† Supplementary data available (No. SUP 56054, 29 pp.): H-atom co-ordinates, thermal parameters, full bond lengths and angles. See Instructions for Authors, *J. Chem. Soc., Dalton Trans.*, 1985, Issue 1, pp. xvii–xix. Structure factors are available from the editorial office.

**Table 1.** Summary of crystal data \*

Complex Formula	(1) [Cu(phen) <sub>2</sub> (O <sub>2</sub> CMe)][ClO <sub>4</sub> ]·2H <sub>2</sub> O	(2) [Cu(phen) <sub>2</sub> (O <sub>2</sub> CMe)][NO <sub>3</sub> ]·2H <sub>2</sub> O	(3) [Zn(phen) <sub>2</sub> (O <sub>2</sub> CMe)][BF <sub>4</sub> ]·2H <sub>2</sub> O
<i>M</i>	618.04	581.024	607.68
Stoichiometry	C <sub>26</sub> H <sub>23</sub> ClCuN <sub>4</sub> O <sub>8</sub>	C <sub>26</sub> H <sub>23</sub> CuN <sub>5</sub> O <sub>7</sub>	C <sub>26</sub> H <sub>23</sub> BF <sub>4</sub> N <sub>4</sub> O <sub>4</sub> Zn
Space group	<i>P</i> 2/ <i>c</i>	<i>P</i> 1	<i>P</i> 2/ <i>c</i>
<i>a</i> /Å	9.671(3)	14.728(2)	9.659(2)
<i>b</i> /Å	8.282(3)	10.499(2)	8.262(2)
<i>c</i> /Å	17.595(4)	8.603(2)	17.651(2)
α/°	90	104.19(5)	90
β/°	109.63(2)	83.97(5)	109.06(5)
γ/°	90	96.81(5)	90
<i>Z</i>	2	2	2
<i>U</i> /Å <sup>3</sup>	1 327.37	1 276.59	1 331.37
<i>D<sub>m</sub></i> /Mg m <sup>-3</sup>	1.53(5)	1.52(5)	1.53(5)
<i>D<sub>c</sub></i> /Mg m <sup>-3</sup>	1.546	1.511	1.516
<i>F</i> (000)	633.98	597.98	616.00
μ/mm <sup>-1</sup>	0.933	0.868	0.957
No. of unique reflections	2 921	4 322	1 819
No. of varied parameters	202	353	202
<i>R</i> = (ΣΔ  <i>F</i> <sub>o</sub>  )	0.0531	0.0606	0.0353
<i>R'</i> = (ΣΔ <i>w</i> <sup>3</sup> /Σ  <i>F</i> <sub>o</sub>   <i>w</i> ) <sup>3</sup>	0.0605	0.0652	0.0384
<i>k</i>	2.9370	2.8265	1.0205
<i>g</i>	0.000 273	0.003 147	0.000 293
Maximum final shift/e.s.d.	0.003	0.002	0.005
Residual electron density	0.76	0.896	0.25
No. of anisotropic atoms	24	39	24

\* Mo-*K*<sub>α</sub> radiation (λ = 0.710 69 Å) used in each case.

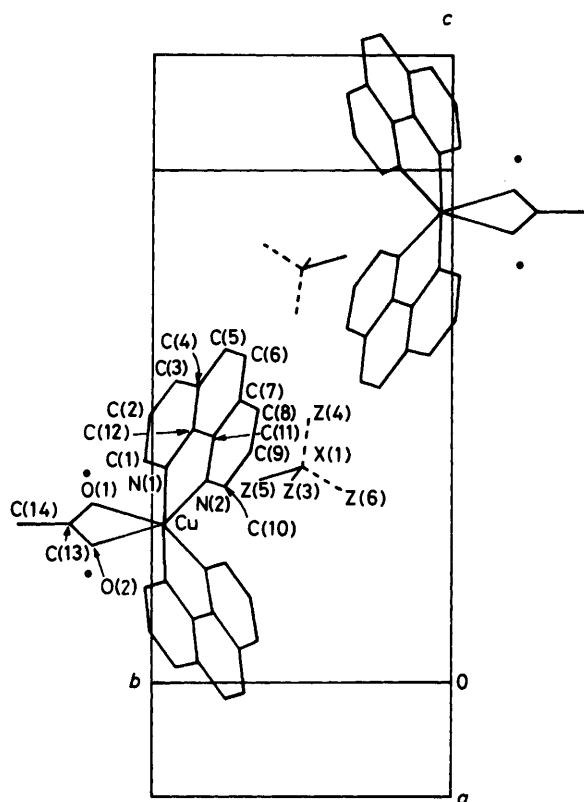


**Figure 1.** Molecular structure (excluding H atoms), atom numbering, and packing diagram for [M(phen)<sub>2</sub>(O<sub>2</sub>CMe)][XZ<sub>4</sub>]·2H<sub>2</sub>O [M = Cu in (1) and Zn in (3); XZ<sub>4</sub> = ClO<sub>4</sub> in (1) and BF<sub>4</sub> in (3)]; H<sub>2</sub>O molecules are shown by ·

anions as ordered groups produced unacceptably high residual peaks and thermal parameters. Both anions were refined as two interpenetrating anions (50% occupancy), which con-

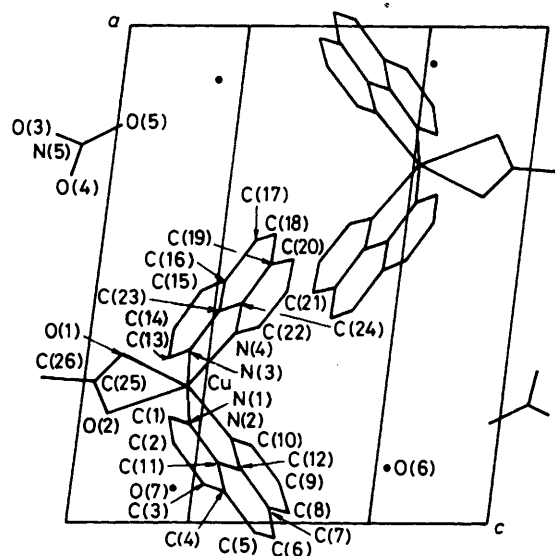


**Figure 2.** Molecular structure (excluding H atoms), atom numbering, and packing diagram for [Cu(phen)<sub>2</sub>(O<sub>2</sub>CMe)][NO<sub>3</sub>]·2H<sub>2</sub>O (2); H<sub>2</sub>O molecules are shown by ·

siderably reduced the residual electron density in the region of these anions, but still retained some rather high thermal parameters and rather short Cl-O and B-F bond distances.

All calculations were carried out with the programs SHELX-76,<sup>8</sup> XANADU (G. M. Sheldrick), ORTEP (C. K. Johnston), and PRETAB (K. Henrick) on IBM 4341 and VAX 11/780 computers. The final atomic co-ordinates for (1)–(3) are given in Table 2, and selected bond lengths and angles in Table 3. Figure 1 shows the local molecular structure of (1) and (3), the atom-numbering scheme used, and the molecular packing. Figure 2 shows the corresponding data for (2).

*Electronic Properties.*—These were recorded as described

**Table 2.** Fractional atomic co-ordinates with estimated standard deviations in parentheses

Atom	x	y	z	Atom	x	y	z
<b>[Cu(phen)<sub>2</sub>(O<sub>2</sub>CMe)][ClO<sub>4</sub>]·2H<sub>2</sub>O (1)</b>							
Cu	0.000 00	0.037 85(6)	0.250 00	C(11)	-0.070 8(3)	0.202 5(3)	0.096 2(1)
N(1)	0.127 5(2)	0.046 5(3)	0.181 2(1)	C(12)	0.070 1(3)	0.134 1(3)	0.111 5(1)
C(1)	0.257 8(3)	-0.024 5(4)	0.195 2(2)	N(2)	-0.136 7(2)	0.178 4(2)	0.152 9(1)
C(2)	0.337 0(3)	-0.010 4(4)	0.141 3(2)	O(1)	-0.094 3(3)	-0.202 9(3)	0.198 5(1)
C(3)	0.281 2(3)	0.078 1(4)	0.072 2(2)	C(13)	0.000 00	-0.281 67(40)	0.250 00
C(4)	0.143 3(3)	0.152 9(3)	0.055 0(2)	C(14)	0.0000	-0.456 2(5)	0.2500
C(5)	0.071 9(4)	0.242 7(3)	-0.017 2(2)	O(2)	-0.379 6(3)	-0.214 7(4)	0.100 1(2)
C(6)	-0.062 6(4)	0.307 2(3)	-0.032 0(2)	Cl(1) *	0.500 00	0.504 20(18)	0.250 00
C(7)	-0.138 7(3)	0.290 1(3)	0.024 5(2)	O(3) *	0.341 3(5)	0.505 8(6)	0.225 5(5)
C(8)	-0.279 4(4)	0.352 0(4)	0.012 4(2)	O(4) *	0.518 1(5)	0.525 5(5)	0.175 6(4)
C(9)	-0.343 9(4)	0.327 3(4)	0.068 7(2)	O(5) *	0.541 9(5)	0.356 8(5)	0.279 2(4)
C(10)	-0.269 6(3)	0.239 6(3)	0.139 2(2)	O(6) *	0.517 4(6)	0.637 1(5)	0.291 7(4)
<b>[Cu(phen)<sub>2</sub>(O<sub>2</sub>CMe)][NO<sub>3</sub>]·2H<sub>2</sub>O (2)</b>							
Cu	0.276 44(3)	0.197 25(4)	0.036 30(5)	C(17)	0.568 4(3)	0.463 4(6)	0.311 2(6)
N(1)	0.200 4(2)	0.023 2(3)	-0.007 0(4)	C(18)	0.584 8(3)	0.345 5(6)	0.332 9(6)
C(1)	0.216 5(3)	-0.084 1(4)	-0.125 9(5)	C(19)	0.522 9(3)	0.230 8(5)	0.280 3(5)
C(2)	0.157 8(4)	-0.201 5(4)	-0.143 1(6)	C(20)	0.534 0(3)	0.104 1(5)	0.302 6(6)
C(3)	0.082 6(3)	-0.207 5(4)	-0.036 9(6)	C(21)	0.470 5(4)	0.001 2(5)	0.250 9(7)
C(4)	0.063 7(3)	-0.098 0(4)	0.086 1(5)	C(22)	0.395 3(3)	0.019 8(4)	0.173 6(6)
C(5)	-0.015 0(3)	-0.092 4(5)	0.201 8(6)	C(23)	0.428 1(3)	0.366 9(4)	0.179 4(4)
C(6)	-0.028 8(3)	0.017 4(6)	0.316 4(6)	C(24)	0.445 3(2)	0.241 0(4)	0.202 8(4)
C(7)	0.033 1(3)	0.134 2(5)	0.330 4(5)	N(4)	0.383 4(2)	0.136 5(3)	0.149 9(4)
C(8)	0.021 8(3)	0.254 0(6)	0.446 8(6)	O(1)	0.340 1(3)	0.161 1(3)	-0.201 5(5)
C(9)	0.083 7(3)	0.362 3(5)	0.445 9(5)	O(2)	0.221 4(3)	0.264 0(4)	-0.187 9(5)
C(10)	0.158 7(3)	0.351 1(4)	0.330 7(5)	C(25)	0.285 7(3)	0.204 4(4)	-0.269 1(4)
C(11)	0.126 3(2)	0.016 6(4)	0.096 7(4)	C(26)	0.292 8(5)	0.186 9(7)	-0.445 6(6)
C(12)	0.110 1(2)	0.133 3(4)	0.219 9(4)	N(5)	-0.238 3(3)	0.228 7(5)	-0.402 5(5)
N(2)	0.172 8(2)	0.241 1(3)	0.219 8(4)	O(3)	-0.216 5(4)	0.330 1(5)	-0.448 3(7)
N(3)	0.352 3(2)	0.371 9(3)	0.104 1(4)	O(4)	-0.301 6(4)	0.155 0(6)	-0.457 6(7)
C(13)	0.334 7(3)	0.487 6(4)	0.082 7(5)	O(5)	-0.201 7(4)	0.209 5(7)	-0.291 2(8)
C(14)	0.392 1(4)	0.603 9(4)	0.134 3(6)	O(6)	0.111 3(3)	0.465 9(4)	0.842 4(5)
C(15)	0.468 7(3)	0.599 2(5)	0.209 4(6)	O(7)	0.074 6(3)	0.551 3(4)	0.173 4(5)
C(16)	0.489 0(3)	0.479 1(4)	0.233 5(5)				
<b>[Zn(phen)<sub>2</sub>(O<sub>2</sub>CMe)][BF<sub>4</sub>]·2H<sub>2</sub>O (3)</b>							
Zn	0.000 00	0.040 40(7)	0.250 00	C(11)	0.073 7(3)	0.140 7(3)	0.107 4(2)
N(1)	0.137 3(2)	0.056 1(3)	0.176 0(1)	C(12)	-0.068 8(3)	0.206 7(3)	0.094 9(2)
C(1)	0.267 4(3)	-0.012 0(4)	0.186 6(2)	N(2)	-0.131 0(3)	0.181 8(3)	0.153 1(1)
C(2)	0.341 6(4)	0.005 0(4)	0.130 9(2)	O(1)	-0.100 9(2)	-0.189 2(3)	0.199 9(1)
C(3)	0.278 6(4)	0.090 7(4)	0.062 5(2)	C(13)	0.0000	-0.266 5(5)	0.2500
C(4)	0.141 4(3)	0.160 8(4)	0.048 4(2)	C(14)	0.0000	-0.445 0(5)	0.2500
C(5)	0.064 3(4)	0.250 2(4)	-0.023 0(2)	O(2)	-0.384 5(3)	-0.234 5(4)	0.105 3(2)
C(6)	-0.069 5(4)	0.312 1(4)	-0.034 4(2)	B(1) *	0.5000	0.502 8(6)	0.2500
C(7)	-0.140 7(4)	0.291 8(4)	0.023 9(2)	F(1) *	0.509 4(6)	0.506 5(6)	0.180 0(4)
C(8)	-0.281 0(4)	0.351 3(4)	0.014 1(2)	F(2) *	0.542 3(7)	0.619 4(7)	0.294 5(5)
C(9)	-0.342 2(4)	0.326 0(4)	0.072 7(2)	F(3) *	0.336 4(6)	0.500 5(7)	0.230 3(5)
C(10)	-0.264 2(3)	0.241 0(4)	0.141 7(2)	F(4) *	0.525 7(7)	0.356 4(6)	0.269 4(6)

\* Two interpenetrating tetrahedra with site occupation factor of 0.5.

previously.<sup>9</sup> Figure 3 shows the effect of temperature on the polycrystalline e.s.r. spectra of (1), [Cu(phen)<sub>2</sub>(O<sub>2</sub>CMe)][BF<sub>4</sub>]·2H<sub>2</sub>O, (5), [Cu(phen)<sub>2</sub>(O<sub>2</sub>CMe)][ClO<sub>4</sub>] (6), and [Cu(phen)<sub>2</sub>(O<sub>2</sub>CMe)][BF<sub>4</sub>] (7). Figure 4 shows the effect of temperature on the e.s.r. spectra of copper(II)-doped (3) and [Zn(phen)<sub>2</sub>(O<sub>2</sub>CMe)][ClO<sub>4</sub>]·2H<sub>2</sub>O. Figure 5 shows the effect of temperature on the single-crystal e.s.r. spectra of (1) and of 10% copper(II)-doped (3). Figure 6 shows the effect of temperature on the single-crystal e.s.r. spectrum of (2) measured in the plane of *g*<sub>3</sub> and *g*<sub>2</sub>. Table 4 summarises the e.s.r. data for the [Cu(phen)<sub>2</sub>(O<sub>2</sub>CMe)]Y series of complexes. Figure 7 summarises the electronic reflectance spectra of the [Cu(phen)<sub>2</sub>(O<sub>2</sub>CMe)]Y series of complexes.

## Results and Discussion

**Crystal Structures.**—The crystal structures of (1)–(3) consist of discrete [M(phen)<sub>2</sub>(O<sub>2</sub>CMe)]<sup>+</sup> cations, a ClO<sub>4</sub><sup>-</sup>, NO<sub>3</sub><sup>-</sup>, or BF<sub>4</sub><sup>-</sup> anion, respectively, and two water molecules of crystallisation. None of the water molecules or the anions are close enough to the copper(II) ion to be considered even weakly semi-co-ordinated.<sup>10</sup> The ClO<sub>4</sub><sup>-</sup> anion in (1) and the BF<sub>4</sub><sup>-</sup> anion in (3) both occupy a special position of two-fold symmetry, and involve considerable disorder<sup>11,12</sup> with relatively high thermal parameters. Consequently, neither is well defined, as previously observed<sup>13</sup> in (5). The NO<sub>3</sub><sup>-</sup> anion in (2) is well ordered and regular in stereochemistry, with N–O distances of 1.217 Å and O–N–O angles of 119.8°, as previously

**Table 3.** Molecular dimensions (bond lengths in Å, angles in °) <sup>a</sup> of the complexes [M(phen)<sub>2</sub>(O<sub>2</sub>CMe)]Y

Complex	(1)	(5) <sup>b</sup>	(2)	(6) <sup>c</sup>	(6) <sup>c,d</sup>	(7) <sup>e</sup>	(3)
M	Cu	Cu	Cu	Cu	Cu	Cu	Zn
Y	ClO <sub>4</sub> <sup>-</sup> ·2H <sub>2</sub> O	BF <sub>4</sub> <sup>-</sup> ·2H <sub>2</sub> O	NO <sub>3</sub> <sup>-</sup> ·2H <sub>2</sub> O	ClO <sub>4</sub> <sup>-</sup>	ClO <sub>4</sub> <sup>-</sup>	BF <sub>4</sub> <sup>-</sup>	BF <sub>4</sub> <sup>-</sup> ·2H <sub>2</sub> O
Space group	<i>P2/c</i>	<i>P2/c</i>	<i>P1</i>	<i>P2<sub>1</sub>/c</i>	<i>P2<sub>1</sub>/c</i>	<i>P1</i>	<i>P2/c</i>
M-N(1)	1.999(2)	2.000(4)	2.000(3)	1.994(4)	2.003(3)	2.010(2)	2.147(2)
M-N(2)	2.122(2)	2.123(4)	2.083(3)	2.098(4)	2.098(3)	2.062(2)	2.116(2)
M-N(3)	1.999(2)	2.000(4)	2.019(3)	2.006(4)	2.013(3)	2.025(2)	2.147(2)
M-N(4)	2.122(2)	2.123(4)	2.170(3)	2.130(4)	2.146(3)	2.218(2)	2.116(2)
M-O(1)	2.252(3)	2.261(5)	2.123(5)	2.220(4)	2.155(4)	1.996(2)	2.184(2)
M-O(2)	2.252(3)	2.261(5)	2.448(5)	2.421(5)	2.532(5)	2.670(3)	2.184(2)
C(25)-O(1)	1.234(3)	1.233(6)	1.225(5)	1.175(6)	1.219(5)	1.252(4)	1.256(3)
C(25)-O(2)	1.234(3)	1.233(6)	1.250(5)	2.166(6)	1.190(5)	1.238(4)	1.256(3)
α <sub>1</sub> ,N(2)-M-O(1)	150.2(2)	149.5(2)	157.7(2)	154.7(2)	154.9(1)	160.5(1)	151.2(1)
α <sub>2</sub> ,N(4)-M-O(1)	95.9(2)	95.4(2)	97.6(1)	91.1(1)	91.5(1)	95.7(1)	94.7(1)
α <sub>3</sub> ,N(2)-M-N(4)	113.4(2)	114.7(2)	104.3(1)	114.1(2)	113.4(1)	103.5(1)	113.0(4)
ΔN <sup>f</sup>	0.0	0.0	0.087	0.132	0.148	0.156	0.0
ΔO <sup>g</sup>	0.0	0.0	0.325	0.201	0.377	0.674	0.0
δ <sup>h</sup>	0.0	0.0	0.429	0.345	0.535	0.845	0.0
Angle O(1) <sup>i</sup>	7	13	16	18	19	42	—
Angle O(2) <sup>i</sup>	7	13	11	25	31	54	—

<sup>a</sup> At 298 K, unless stated otherwise. <sup>b</sup> From ref. 13. <sup>c</sup> From ref. 6. <sup>d</sup> At 173 K. <sup>e</sup> From ref. 20. <sup>f</sup> ΔN = Cu-N(4) - Cu-N(2). <sup>g</sup> ΔO = Cu-O(2) - Cu-O(1). <sup>h</sup> δ = ΔN + ΔO + [Cu-N(3) - Cu-N(1)]. <sup>i</sup> Angle O(1) [O(2)] = angle which the major axis of the thermal ellipsoid of O(1) [O(2)] makes to the Cu-O(1) [O(2)] direction.

**Table 4.** E.s.r. spectra of [M(phen)<sub>2</sub>(O<sub>2</sub>CMe)]Y complexes

Complex	Type <sup>a</sup>	% Cu	Temp. <sup>b</sup>	g <sub>1</sub> <sup>c</sup>	g <sub>2</sub> <sup>c</sup>	g <sub>3</sub> <sup>c</sup>	10 <sup>4</sup> A <sub>3</sub> /cm <sup>-1</sup> ,
(1)	p.c.	100	r.t.	2.028	—	2.223	—
(1)	p.c.	100	l.t.	2.032	2.083	—	—
(1)	s.c.	100	r.t.	2.026	2.200	2.213	—
(1)	s.c.	100	l.t.	(2.03)	(2.10)	(2.25)	—
Cu-doped [Zn(phen) <sub>2</sub> (O <sub>2</sub> CMe)][ClO <sub>4</sub> ·2H <sub>2</sub> O]	p.c.	10	r.t.	—	—	2.210	94
Cu-doped [Zn(phen) <sub>2</sub> (O <sub>2</sub> CMe)][ClO <sub>4</sub> ·2H <sub>2</sub> O]	p.c.	10	l.t.	—	2.087	2.275	166
(5)	p.c.	100	r.t.	2.035	—	2.220	—
(5)	p.c.	100	l.t.	2.050	2.083	2.260	—
Cu-doped (3)	p.c.	10	r.t.	2.050	—	2.213	92
Cu-doped (3)	p.c.	10	l.t.	—	2.085	2.260	166
Cu-doped (3)	s.c.	10	r.t.	2.022	2.210	2.214	84
Cu-doped (3)	s.c.	10	l.t.	(2.02)	(2.15)	(2.26)	165
(6)	p.c.	100	r.t.	2.040	—	2.200	—
(6)	p.c.	100	l.t.	—	2.082	—	—
(6)	s.c.	100	r.t.	2.027	2.168	2.212	—
(7)	p.c.	100	r.t.	2.060	2.105	2.260	—
(7)	p.c.	100	l.t.	2.065	2.087	2.280	—
(7)	s.c.	100	r.t.	2.054	2.106	2.266	—

<sup>a</sup> p.c. = Polycrystalline; s.c. = single crystal. <sup>b</sup> r.t. = Room temperature; l.t. = low temperature (77 K). <sup>c</sup> Values are ±0.001; values in parentheses are ±0.01.

observed.<sup>14</sup> In (1) and (3) the [M(phen)<sub>2</sub>(O<sub>2</sub>CMe)]<sup>+</sup> cation is six-co-ordinate with a near regular *cis*-octahedral MN<sub>4</sub>O<sub>2</sub> chromophore, as the M atom occupies a crystallographic two-fold position, and the space groups are isomorphous, Table 1. As the zinc(II) ion of (3) is spherically symmetrical (with a *d*<sup>10</sup> configuration), while the copper(II) is non-spherically symmetrical (*d*<sup>9</sup> configuration<sup>9</sup>), there are significant differences in the local chromophore stereochemistry. The out-of-plane M-N(1) distances are 1.999(2) and 2.147(2) Å in (1) and (3), respectively. The in-plane M-N(2) distances are just significantly different, 2.122(2) and 2.116(2) Å, respectively, while the M-O(1) distances are very different, 2.252(3) and 2.184(2) Å, respectively. Thus, while the metal-ligand distances in the ZnN<sub>4</sub>O<sub>2</sub> chromophore involve a spread of only 0.07 Å, the spread in the CuN<sub>4</sub>O<sub>2</sub> chromophore is considerably larger, 0.25 Å. The difference in the in-plane M-O(1) and M-N(2) distance in the Cu chromophore, 0.13 Å, is nearly twice that in the Zn chromophore (0.07 Å). This difference

justifies the *cis*-distorted-octahedral description for the CuN<sub>4</sub>O<sub>2</sub> chromophore of (1), as introduced earlier for (4),<sup>15,16</sup> relative to the nearer regular *cis*-octahedral stereochemistry in (3). The lattice water molecules are within hydrogen-bonding distance of the O(1) atom, at 2.72 and 2.73 Å, in (1) and (3) respectively.

In (2) the stereochemistry of the CuN<sub>4</sub>O<sub>2</sub> chromophore is basically five-co-ordinate with a second oxygen of the acetate group occupying a sixth co-ordinating position at a distance >2.4 Å to give a (4 + 1 + 1\*) type co-ordination.<sup>17</sup> The CuN<sub>4</sub>O<sub>2</sub> chromophore involves a distorted stereochemistry,<sup>4</sup> intermediate between trigonal bipyramidal and square pyramidal, with the distortion related to the regular *cis*-octahedral stereochemistry of (1) by the sense of the 'structural pathway,'<sup>18</sup> for the [Cu(bipy)<sub>2</sub>(OXO)]Y complexes.<sup>4,19</sup> The detailed geometry of the CuN<sub>4</sub>O<sub>2</sub> chromophore of (2) is then closely comparable<sup>6</sup> to that in (6), and to the more asymmetric distortion<sup>20</sup> of (7), see Table 3. In (2) the O(6)

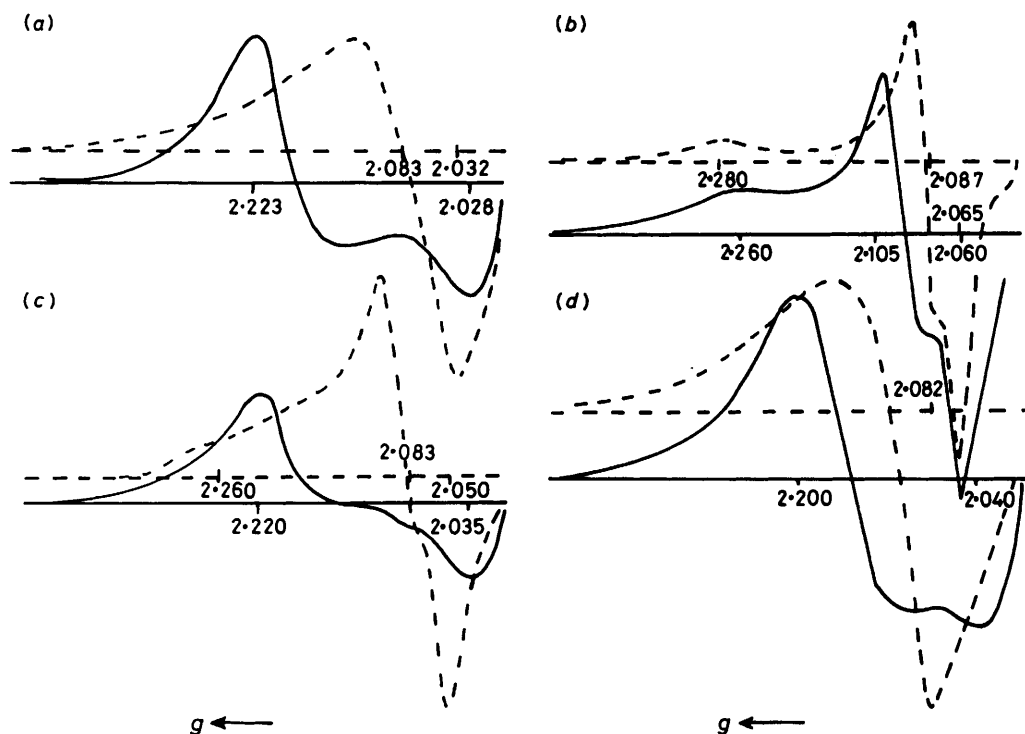


Figure 3. Polycrystalline e.s.r. spectra at room temperature (—) and at 77 K (---) of (a) (1), (b) (7), (c) (5), and (d) (6)

water is within hydrogen bonding distance of the O(2) atom.

The series of complexes (1), (5), (2), (6), and (7), Table 3, represents a sequence of cation distortion isomers<sup>21</sup> of increasing asymmetry; the structure of (6) has already been reported as temperature variable.<sup>6</sup> The primary purpose of this paper is to examine the electronic properties of this series of cation distortion isomers in the context of this fluxional behaviour.<sup>3</sup>

**E.S.R. Spectra.**—The polycrystalline e.s.r. spectra of (1), (5), and (6) are anisotropic at room temperature, Figure 3, and show significant change with decreasing temperature. In (1) and (5) the room-temperature spectra are axial<sup>9</sup> ( $g_{\perp} > g_{\parallel} \approx 2.0$ ) consistent with the compressed  $\text{CuN}_4\text{O}_2$  chromophore present, and change to an axially elongated form at low temperature ( $g_{\perp} \gg g_{\parallel} > 2.0$ ), but with  $g_{\parallel}$  not clearly defined. The same type of change occurs in (6), but as the  $\text{CuN}_4\text{O}_2$  chromophores are misaligned<sup>9</sup> the observed  $g$  values do not equate with the local molecular  $g$  values. The spectrum of (7), Figure 3, is clearly rhombic at room temperature ( $g_3 \gg g_2 > g_1 > 2.0$ ) consistent with the elongated ( $4 + 1 + 1^*$ ) structure<sup>22</sup> of the  $\text{CuN}_4\text{O}_2$  chromophore and, predictably, shows little change with temperature. The e.s.r. spectra of the copper(II)-doped  $[\text{Zn}(\text{phen})_2(\text{O}_2\text{CMe})\text{Y}]$  ( $\text{Y} = \text{ClO}_4^- \cdot 2\text{H}_2\text{O}$  or  $\text{BF}_4^- \cdot 2\text{H}_2\text{O}$ ), Figure 4, show clear copper hyperfine structure and change even more significantly with decreasing temperature, with  $g$  values again changing in form from ( $g_{\perp} \gg g_{\parallel} > 2.0$ ) to ( $g_{\parallel} \gg g_{\perp} > 2.0$ ). The similarity of the  $g$  values and their changes with decreasing temperature suggest that the stereochemistry of the  $\text{CuN}_4\text{O}_2$  chromophore does not change significantly with dilution in the zinc host lattice.<sup>22</sup> This suggestion is supported by the lack of energy change of the electronic spectra<sup>22</sup> in these copper-doped systems (see later), and the similarity of this situation in the copper(II)-doped  $[\text{Zn}(\text{bipy})_2(\text{ONO})][\text{NO}_3]$  system.<sup>4</sup> Figure 5(b) shows the

effect of temperature on the single-crystal e.s.r. spectrum of the 10% copper(II)-doped (3) system measured in the  $\text{Cu}, \text{N}(2), \text{N}(4), \text{O}(1), \text{O}(2)$  plane. At room temperature the spectrum is isotropic, showing four Cu hyperfine lines, and almost independent of the direction. At liquid-nitrogen temperature, up to eight lines are observed, consistent<sup>4</sup> with the presence of two magnetic centres, whose maximum  $g$  values (Table 4) correspond to the directions of the Cu-O(1) and Cu-N(4) bonds in the measured plane. The single-crystal e.s.r. spectrum of (1) measured in the same plane shows a single  $g$  value, which varies significantly with angle, and which splits into two magnetic centres at 77 K, Figure 5(a),  $g_3 = 2.25$  and  $g_2 = 2.10$ . This magnetic behaviour is consistent with the formation of two crystal domains at low temperature or a change in phase.<sup>23</sup> The crystal structure of (2) was determined to avoid this problem, as it crystallises in the triclinic space group  $P1$  and the two  $\text{CuN}_4\text{O}_2$  chromophores are aligned. Figure 6 shows the single-crystal e.s.r. spectrum of (2) measured in the  $\text{Cu}, \text{N}(2), \text{N}(4), \text{O}(1), \text{O}(2)$  plane. Only a single magnetic centre is observed at any temperature. There is a significant change in  $g$  value with temperature, Figure 6, and also a small change in direction with decreasing temperature. This behaviour in (2) suggests that the observation of two magnetic centres in copper-doped (3) and in (1) arises from a change of phase rather than the presence of two magnetic domains. Some evidence for the change of phase was observed in single crystals of (1), which turned opaque on cooling to liquid-nitrogen temperature and shattered on returning to room temperature. This prevented the low-temperature X-ray crystal structure determination of (1).<sup>24</sup> Differential thermal analysis of (1) down to 77 K showed a discontinuity at ca. 223 K, consistent with a possible phase change at this temperature. The extrapolation of the single-crystal  $g$  factors, Figure 6, to 0 K yields approximate  $g$  values of 2.300, 2.078, and 2.057, i.e. nearly axial and consistent with the predicted

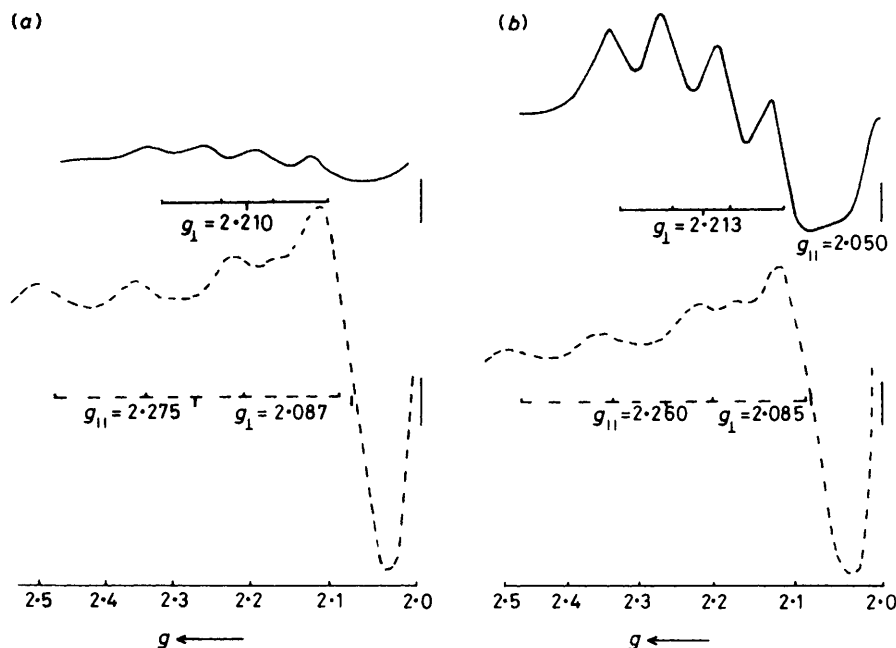


Figure 4. Polycrystalline e.s.r. spectra at room temperature (—) and 77 K (---) of 10% copper(II)-doped complexes (a)  $[\text{Zn}(\text{phen})_2(\text{O}_2\text{CMe})][\text{ClO}_4]\cdot 2\text{H}_2\text{O}$  and (b) (3)

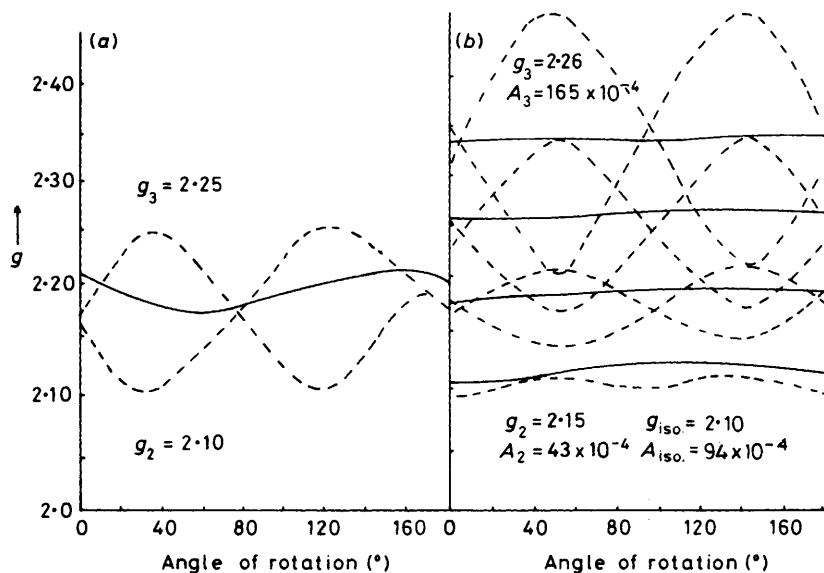


Figure 5. Single-crystal e.s.r. spectra at room temperature (—) and 77 K (---) of (a)  $[\text{Cu}(\text{phen})_2(\text{O}_2\text{CMe})][\text{ClO}_4]\cdot 2\text{H}_2\text{O}$  and (b) 10% copper(II)-doped  $[\text{Zn}(\text{phen})_2(\text{O}_2\text{CMe})][\text{BF}_4]\cdot 2\text{H}_2\text{O}$ ; both were measured in the Cu,N(2),N(4),O(1),O(2) plane; values of  $A$  are in  $\text{cm}^{-1}$

elongated square-pyramidal distorted ( $4 + 1 + 1^*$ )  $\text{CuN}_4\text{O}_2$  chromophore. The temperature variation of the  $g$  values, Figure 6, yields a  $\Delta E$  value of  $132 \pm 20 \text{ cm}^{-1}$ , reasonably comparable to the value of  $168 \pm 20 \text{ cm}^{-1}$  obtained from the structural data for (6), Table 3. The non-variable-temperature e.s.r. spectrum of (7) is then consistent with the more extreme distorted ( $4 + 1 + 1^*$ ) structure present which may only involve a small amount of residual fluxional behaviour, and represents the near-static distorted stereochemistry of the underlying  $\text{CuN}_4\text{O}_2$  chromophore.

**Electronic Spectra.**—The electronic spectra of all five  $[\text{Cu}(\text{phen})_2(\text{O}_2\text{CMe})]\text{Y}$  complexes, Figure 7, consist of two clearly resolved peaks at ca. 10 000 and 14 000  $\text{cm}^{-1}$ . The

energies are the same for the isomorphous pair (1) and (5) (9 500 and 13 700  $\text{cm}^{-1}$ ), but both bands show significant differences for (6), (2), and (7) (10 300 and 13 500, 9 640 and 14 200, 10 400 and 14 500  $\text{cm}^{-1}$  respectively). The near comparability of the electronic spectra of this series of cation distortion isomers, despite the seemingly different  $\text{CuN}_4\text{O}_2$  chromophore structures present, Table 3, can be understood if the  $\text{CuN}_4\text{O}_2$  chromophores are subject to fluxional behaviour,<sup>3</sup> as has been suggested for the  $[\text{Cu}(\text{bipy})_2(\text{ONO})]\text{Y}$  series of complexes and confirmed in the low-temperature structure of (4). As the lifetimes<sup>25</sup> of the electronic spectra are short,  $10^{-15} \text{ s}$ , the observed transitions relate to the extreme stereochemistry of the underlying static ( $4 + 1 + 1^*$ )  $\text{CuN}_4\text{O}_2$  chromophore geometry, as approximately observed in (7),

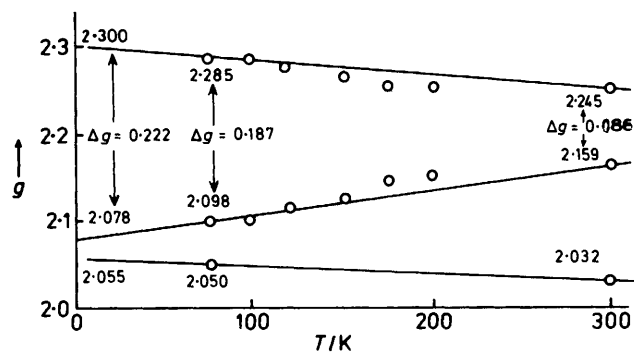


Figure 6. Temperature variation of the single-crystal  $g$  values for  $[\text{Cu}(\text{phen})_2(\text{O}_2\text{CMe})][\text{NO}_3]\cdot 2\text{H}_2\text{O}$ ;  $\Delta g = g_3 - g_2$

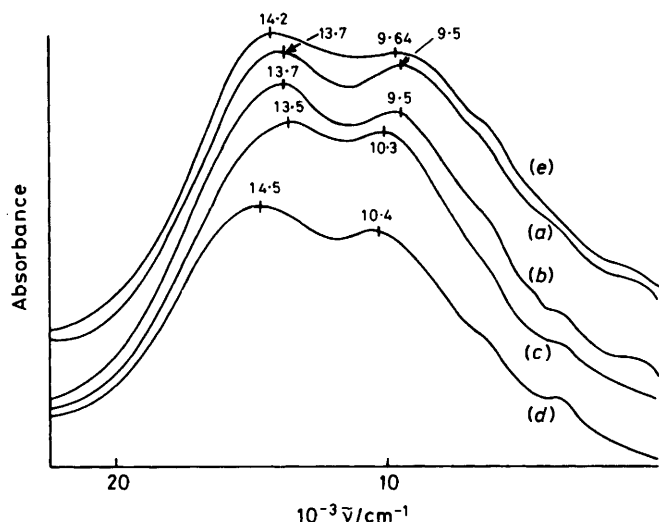


Figure 7. Electronic reflectance spectra of  $[\text{Cu}(\text{phen})_2(\text{O}_2\text{CMe})]\text{Y}$  complexes: (a) (1); (b) (5); (c) (6); (d) (7); (e) (2)

and not to the pseudo-geometry observed by  $X$ -ray crystallography which yields a time-averaged structure. The small differences that are observed in Figure 7 then relate to small differences in the structures of the underlying static geometries of the  $\text{CuN}_4\text{O}_2$  chromophores, which arise due to the different lattice environments of the  $[\text{Cu}(\text{phen})_2(\text{O}_2\text{CMe})]^+$  cations in these cation distortion isomers, as a consequence of the 'plasticity effects'.<sup>26</sup> It has already been demonstrated<sup>27</sup> that the effect of reducing the temperature on the fluxional  $\text{CuN}_4\text{O}_2$  chromophore of (4) produces a linear correlation between the  $\text{Cu}-\text{O}(1)$  and  $\text{Cu}-\text{O}(2)$  distances. If the corresponding distances for the  $[\text{Cu}(\text{phen})_2(\text{O}_2\text{CMe})]\text{Y}$  complexes are similarly plotted, Figure 8, there is no simple correlation between the  $\text{Cu}-\text{O}(1)$  and  $\text{Cu}-\text{O}(2)$  distances for all the phen complexes. The best correlation is through the data for (1), (5), (2), and (7), with those for (6) significantly different, and suggest that the underlying static stereochemistry of (1), (5), (2), and (7) will not be significantly different. The best correlation is then approximately parallel to the line drawn between the 298 and 173 K data points<sup>6</sup> for (6), which is known to involve a fluxional stereochemistry, but with a significantly different underlying static stereochemistry to the complexes involved in the best correlation above.

The electronic reflectance spectra of copper(II)-doped (3) are independent of concentration of the copper(II) ion, as previously established<sup>4</sup> for the copper(II)-doped  $[\text{Zn}(\text{bipy})_2(\text{ONO})][\text{NO}_3]$  system. Thus, despite the significant difference

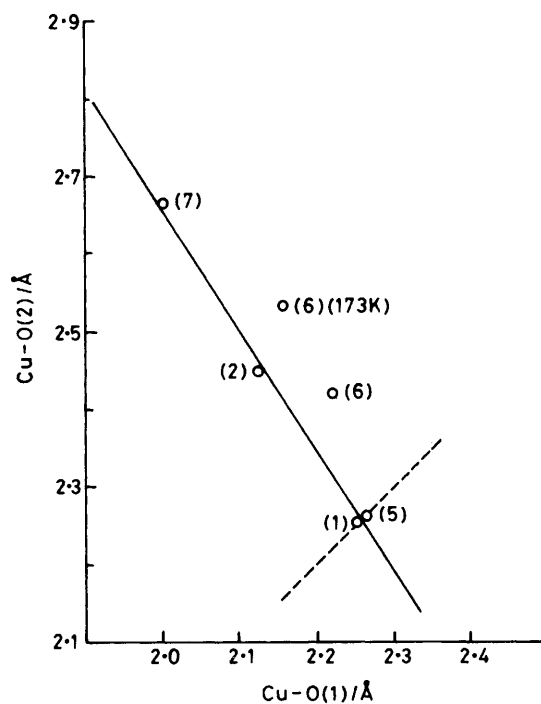


Figure 8.  $\text{Cu}-\text{O}(2)$  versus  $\text{Cu}-\text{O}(1)$  distances (298 K) for  $[\text{Cu}(\text{phen})_2(\text{O}_2\text{CMe})]\text{Y}$  complexes

between the local  $\text{MN}_4\text{O}_2$  chromophores of (5) and (3), the geometry of the  $\text{CuN}_4\text{O}_2$  chromophore in (3) is unaffected by the  $\text{ZnN}_4\text{O}_2$  stereochemistry. This is a further example of the 'non-co-operative Jahn-Teller effect'<sup>22</sup> in this series of molecular-type lattices, and it justifies equating the e.s.r. spectra of the 10% copper(II)-doped (3) systems with the structure of pure (3).

**Thermal Parameters.**—The use of the thermal parameter data<sup>28</sup> of the oxygen ligands as evidence of fluxional behaviour in these *cis*-octahedral chromophores has previously been suggested.<sup>13,19</sup> Figure 9 restricts the data to the Cu, N(2), N(4), acetate carbon and oxygen atoms in  $[\text{M}(\text{phen})_2(\text{O}_2\text{CMe})]^+$  cation complexes. The data for (3) clearly show that the thermal ellipsoids of O(1) and O(1') are spherical and that there is no disorder or fluxional behaviour involved with the  $\text{ZnN}_4\text{O}_2$  chromophore associated with the two-fold special position of the  $P2/c$  space group. In the corresponding copper(II) complexes (1) and (5)<sup>15</sup> there is maximum eccentricity<sup>13</sup> in the thermal ellipsoids of O(1) and O(1') with the major axes lying close to the  $\text{Cu}-\text{O}(1)$  direction: 8 and 13° in (1) and (5), respectively. In contrast, the thermal ellipsoids for the oxygen atoms of (2) reflect an intermediate situation, Figure 9, with the ellipsoids for the short-bonded O(1) atom essentially spherical, but those for the long-bonded O(2) atom are more elliptical with the major axis at a significant angle (16°) to the  $\text{Cu}-\text{O}(2)$  direction.

**Fluxional Model.**—The present paper completes the data on a series of  $[\text{Cu}(\text{bipy})_2(\text{ONO})]\text{Y}$  and  $[\text{Cu}(\text{phen})_2(\text{O}_2\text{CMe})]\text{Y}$  complexes characterised by the following features. (i) They form a series of structures varying from regular *cis*-distorted octahedral to distorted (4 + 1 + 1\*) structures, with  $\delta$  varying from 0.0–0.845 Å. (ii) The geometry of the  $\text{CuN}_4\text{O}_2$  chromophore is temperature dependent;  $\delta$  varies from 0.11 to 0.61 Å in (4) and from 0.345 to 0.535 Å in (6), with  $\delta = [\text{Cu}-\text{O}(2) - \text{Cu}-\text{O}(1)] + [\text{Cu}-\text{N}(4) - \text{Cu}-\text{N}(2)] + [\text{Cu}-\text{N}(3) - \text{Cu}-\text{N}(1)]$ . (iii) The e.s.r. spectra are temperature

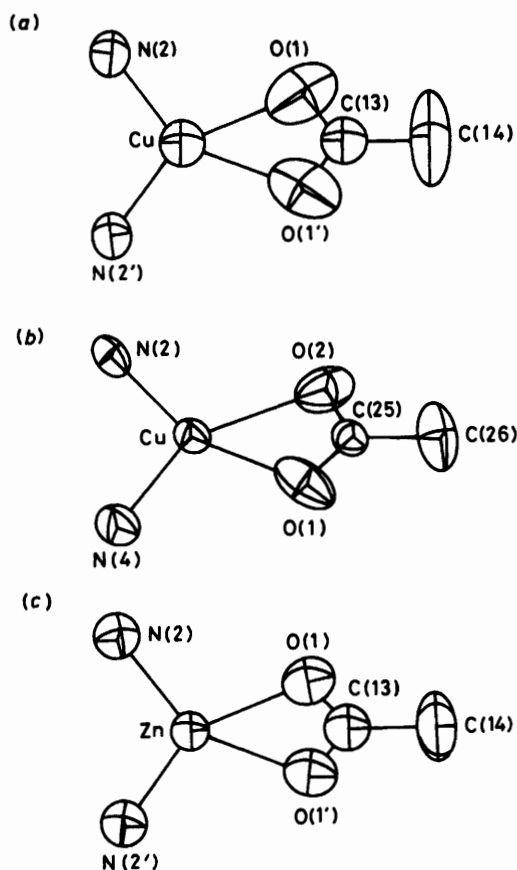


Figure 9. Thermal ellipsoid plots for the in-plane  $\text{CuN}_4\text{O}_2$  chromophores of (a)  $[\text{Cu}(\text{phen})_2(\text{O}_2\text{CMe})][\text{ClO}_4]\cdot 2\text{H}_2\text{O}$ ; (b)  $[\text{Cu}(\text{phen})_2(\text{O}_2\text{CMe})][\text{NO}_3]\cdot 2\text{H}_2\text{O}$ ; (c)  $[\text{Zn}(\text{phen})_2(\text{O}_2\text{CMe})][\text{BF}_4]\cdot 2\text{H}_2\text{O}$

variable, changing from ( $g_{\perp} \gg g_{\parallel} \approx 2.0$ ) at room temperature to  $g_1 \gg g_2 \approx g_3 > 2.0$  at low temperature, with the main temperature variation restricted to the two-dimensional  $\text{Cu}$ ,  $\text{N}(2)$ ,  $\text{N}(4)$ ,  $\text{O}(1)$ ,  $\text{O}(2)$  plane. (iv) The electronic reflectance spectra are nearly structure invariant. (v) Isomorphous zinc(II) and copper(II) complexes exist in which the  $\text{ZnN}_4\text{O}_2$  and  $\text{CuN}_4\text{O}_2$  chromophores are not isostructural, and the former involve a near regular *cis*-octahedral structure.

As there are non-equivalent ligands present a description of these effects in terms of a genuine Jahn-Teller effect<sup>3,28,29</sup> is inappropriate, and it is necessary to use the energy diagram appropriate to the pseudo-Jahn-Teller effect<sup>2,13,29</sup> Figure 10.

An important question with the pseudo-Jahn-Teller effect is whether or not it is large enough<sup>30</sup> to produce the magnitudes of the bond-length distortions observed. If not, the  $\text{CuN}_4\text{O}_2$  chromophore must be considered to have a near degenerate non-rigid stereochemistry, which can be described [see Figure 4(b) of ref. 31] by an adiabatic potential-energy surface identical in appearance to that of Figure 10(a) and (b). This diagram equally accounts for the properties described in this section and it is only the origin of the diagram that is in question. As the historical development of the stereochemistry of copper(II) has been associated, traditionally<sup>9</sup> with the Jahn-Teller effect, we prefer the pseudo-Jahn-Teller origin of Figure 10.

Owing to the non-equivalent ligands present, the two potential-energy surfaces are separated at the origin by  $2\Delta^1$  (see Figure 9 of ref. 29), and of necessity have different symmetry,  ${}^2A$  or  ${}^2B$ . In general a single degenerate mode is involved in the vibronic coupling<sup>29</sup> which must have *b*

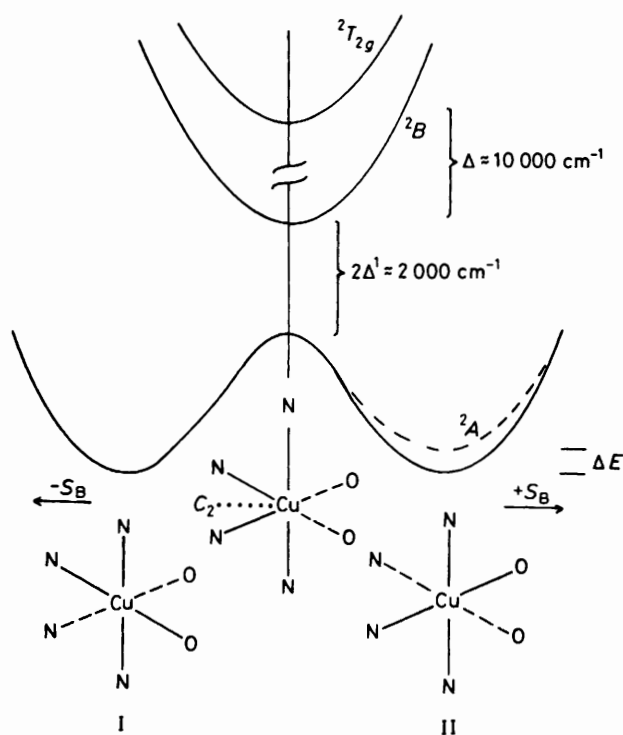


Figure 10. Pseudo-Jahn-Teller potential-energy surface  $\text{CuN}_4\text{O}_2$  chromophore: (a) (—) equivalent wells; (b) (---) non-equivalent wells

symmetry in order to produce a non-zero second-order Jahn-Teller coupling between the two potential-energy surfaces.<sup>2</sup> The form of the active mode then relates closely to the extreme sense of distortion of the  $(4 + 1 + 1^*)$  geometry,<sup>20</sup> as in (7) ( $S_{2b}$ ),<sup>4</sup> Figure 10, which relates to the regular *cis*-distorted octahedral  $\text{CuN}_4\text{O}_2$  chromophore ( $C_2$  symmetry) to the square-pyramidal distorted  $(4 + 1 + 1^*)$  structure, via the 'structural pathway'<sup>4,18</sup> (see Figure 8 of ref. 4). The diagram in Figure 10(a) involves equal energies for wells I and II, and hence equivalent thermal populations, corresponding to a  $\text{CuN}_4\text{O}_2$  chromophore of  $C_2$  symmetry, as in (1) and (5), which can only occur in a high-symmetry lattice.<sup>23</sup> In general, the energies of wells I and II are not equivalent and differ by  $\Delta E$ , Figure 10(b), which if less than thermal energy results in a different thermal population (*n*) of wells I and II, with  $n_I > n_{II}$ . Consequently the observed  $\text{CuN}_4\text{O}_2$  geometry will be a weighted average of the populations of wells I and II, as in (2), and will be temperature variable as observed<sup>6</sup> for (6). As the lifetime<sup>25</sup> for the measurement of the e.s.r. spectra is long ( $10^{-9}$  s) compared with that of the electronic spectra ( $10^{-15}$  s) the e.s.r. spectra will also be temperature variable as observed above, but the electronic spectra will be almost structure invariant as they relate to the underlying static  $\text{CuN}_4\text{O}_2$  chromophore stereochemistry. Figure 10(a) and (b) adequately accounts for the different stereochemistries and electronic properties of this series of  $[\text{Cu}(\text{phen})_2(\text{O}_2\text{CMe})]\text{Y}$  cation distortion isomers.

#### Acknowledgements

We acknowledge the award of a senior demonstratorship from U.C.C. (to W. F.), help in data collection from Drs. P. G. Owston, M. McPartlin, and K. Henrick (The Polytechnic of North London, Holloway), the Computer Bureau, U.C.C., for computing facilities, Drs. G. M. Sheldrick and S. Motherwell



(Cambridge University) and K. Henrick (Polytechnic of North London) for the use of their programs, the Micro-analysis Section, U.C.C., for analysis, and Dr. P. O'Brien (Chelsea College, London) for the thermal analysis data.

### References

- 1 C. J. Simmons, A. Clearfield, W. Fitzgerald, S. Tyagi, and B. J. Hathaway, *J. Chem. Soc., Chem. Commun.*, 1983, 189.
- 2 C. J. Simmons, A. Clearfield, W. Fitzgerald, S. Tyagi, and B. J. Hathaway, *Inorg. Chem.*, 1983, **22**, 2463.
- 3 B. J. Hathaway, M. Duggan, A. Murphy, J. Mullane, C. Power, A. Walsh, and B. Walsh, *Coord. Chem. Rev.*, 1981, **36**, 271.
- 4 W. Fitzgerald, B. Murphy, S. Tyagi, A. Walsh, B. Walsh, and B. J. Hathaway, *J. Chem. Soc., Dalton Trans.*, 1981, 2271.
- 5 F. Clifford, E. Counihan, W. Fitzgerald, K. Seff, C. J. Simmons, S. Tyagi, and B. J. Hathaway, *J. Chem. Soc., Chem. Commun.*, 1982, 196.
- 6 C. J. Simmons, M. Lundeen, K. Seff, N. Alcock, W. Fitzgerald, and B. J. Hathaway, *Acta Crystallogr., Sect. C*, in the press.
- 7 D. T. Cromer and D. Liberman, *J. Chem. Phys.*, 1970, **53**, 1891; D. T. Cromer and J. B. Mann, *Acta Crystallogr., Sect. A*, 1968, **24**, 321.
- 8 G. M. Sheldrick, SHELX-76 a program for crystal structure determination, University of Cambridge, 1976.
- 9 B. J. Hathaway and D. E. Billing, *Coord. Chem. Rev.*, 1970, **5**, 143.
- 10 I. M. Procter, B. J. Hathaway, and P. Nicholls, *J. Chem. Soc. A*, 1968, 1678.
- 11 H. C. Stynes and J. A. Ibers, *Inorg. Chem.*, 1971, **10**, 2304.
- 12 B. J. Kilbourne, R. R. Ryan, and J. D. Dunitz, *J. Chem. Soc. A*, 1969, 2407.
- 13 C. J. Simmons, K. Seff, F. Clifford, and B. J. Hathaway, *Acta Crystallogr., Sect. C*, 1983, **39**, 1360.
- 14 C. C. Addison, N. Logan, S. C. Wallwork, and C. D. Garner, *Q. Rev. Chem. Soc.*, 1971, **25**, 289.
- 15 I. M. Procter, B. J. Hathaway, D. E. Billing, R. J. Dudley, and P. Nicholls, *J. Chem. Soc. A*, 1969, 1192.
- 16 F. S. Stephens and I. M. Procter, *J. Chem. Soc. A*, 1969, 1248.
- 17 B. J. Hathaway, *Struct. Bonding (Berlin)*, 1973, **14**, 49.
- 18 H. B. Burgi, *Angew. Chem., Int. Ed. Engl.*, 1975, **14**, 460; J. D. Dunitz, 'X-Ray Analysis and Structure of Organic Molecules,' Cornell University Press, London, 1979, ch. 7.
- 19 A. Walsh, B. Walsh, B. Murphy, and B. J. Hathaway, *Acta Crystallogr., Sect. B*, 1981, **37**, 1512.
- 20 W. Fitzgerald and B. J. Hathaway, *Acta Crystallogr., Sect. C*, 1984, **40**, 243.
- 21 N. Ray, L. Hulett, R. Sheahan, and B. J. Hathaway, *Inorg. Nucl. Chem. Lett.*, 1978, **14**, 305.
- 22 M. Duggan, M. Horgan, J. Mullane, P. C. Power, N. Ray, A. Walsh, and B. J. Hathaway, *Inorg. Nucl. Chem. Lett.*, 1980, **16**, 407.
- 23 D. Reinen and C. Freibell, *Struct. Bonding (Berlin)*, 1979, **37**, 1.
- 24 P. O'Brien, personal communication.
- 25 E. L. Muetterties, *Inorg. Chem.*, 1965, **4**, 795.
- 26 J. Gazo, I. B. Bersuker, J. Garaj, M. Kabesova, J. Kohout, M. Langfelderova, M. Melnik, M. Seraton, and F. Valach, *Coord. Chem. Rev.*, 1976, **11**, 253.
- 27 S. Tyagi and B. J. Hathaway, unpublished work.
- 28 J. A. Ammeter, H. Burgi, E. Gamp, V. Meyer-Sandrin, and W. P. Jensen, *Inorg. Chem.*, 1979, **18**, 733.
- 29 I. B. Bersuker, *Coord. Chem. Rev.*, 1975, **14**, 357 and refs. therein.
- 30 R. Boca, personal communication.
- 31 J. H. Ammeter, *Nouv. J. Chim.*, 1980, **4**, 631.

Received 10th February 1984; Paper 4/243